J Electr Eng Technol.2017; 13(?): 1921-718
http://doi.org/10.???/JEET.2017.13.1.1921

ISSN(Print) 1975-0102
ISSN(Online) 2093-7423

# Chaos Suppression in Fractional order Permanent Magnet Synchronous Generator in Wind Turbine Systems

**Karthikeyan Rajagopal†, Anitha Karthikeyan* and Prakash Duraisamy****

**Abstract** – In this paper we investigate the control of three-dimensional non-autonomous fractional-order uncertain model of a permanent magnet synchronous generator (PMSG) via a adaptive control technique. We derive a dimensionless fractional order model of the PMSM from the integer order presented in the literatures. Various dynamic properties of the fractional order model like Eigen values, Lyapunov exponents, bifurcation and bicoherence are investigated. The system chaotic behavior for various orders of fractional calculus are presented. Nonlinear adaptive controllers and adaptive sliding mode controllers are derived to suppress the chaotic oscillations of the fractional order model. As the direct Lyapunov stability analysis of the robust controller is difficult for a fractional order first derivative, we have derived a new lemma to analyze the stability of the system. Numerical simulations of the proposed chaos suppression methodology are given to prove the analytical results derived through which we show that for the derived adaptive controller and the parameter update law, the origin of the system for any bounded initial conditions is asymptotically stable.

**Keywords**: Chaos suppression, Fractional order systems, Permanent magnet synchronous generator, Bifurcation, Lyapunov stability, LabVIEW, FPGA



## 1. Introduction

The renewable nature and their reduced environmental impact, Wind energy plays an important role in the present and future power generation methods. Control mechanism of the Permanent Magnet Synchronous Generators (PMSG) coupled with the wind turbines are of high complexity. Several control strategies of these control mechanisms are investigated by Robinson et al [1]. Most of the Wind Energy Generators operate at fixed speed except the initializing phase [2]. Fixed Speed of operation guarantees a high coefficient of performance and these speed are often fixed for Wind turbines. To operate turbines at these speeds one has to control the Non-Linearity of the speed components [3].

Permanent Magnet Synchronous Motors (PMSG) are the most preferred generation systems for Wind energy conversions. The chaotic behavior in the permanent magnet synchronous generator for wind turbine system is investigated, and the Active Disturbance Rejection Control (ADRC) strategy is proposed to suppress chaotic behavior and make operating stably [4]. The use of a predictive control strategy which was investigated with a one point controller of PMSG is studied and this control mechanism used Genetic Algorithms to to estimate the optimal parameter values of the wind turbine leads to maximization of the power generation [5]. PMSG system controlled by the online-tuned parameters of the novel modified recurrent wavelet neural network (NN)-controlled system is proposed to control output voltages and powers of controllable rectifier and inverter [6].

The performance of the PMSM is sensitive to system parameter and external load disturbance in the plant. Some investigations, for example, by Li et al. [7] and Jing et al. [8] show that with certain parameter values, the PMSM displays chaotic behavior. It is found that with the help of fractional derivatives, many systems in interdisciplinary fields can be elegantly described. [7-9]. Furthermore many integer order chaotic systems of fractional order have been studied widely. [10-14]. All the physical phenomena in nature exist in the form of fractional order, [15] integer order (classical) differential equation is just a special case of fractional differential equation. The importance of fractional-order models is that they can yield a more accurate description and give a deeper insight into the physical processes underlying a long range memory behavior.

Chaos modelling have applications in many areas in science and engineering [15-17]. Some of the common applications of chaotic systems in science and engineering are chemical reactors, brusselators, dynamos, Tokamak systems, biology models, neurology, ecology models, memristive devices, etc. An analysis of saddle-node and Hopf bifurcations in indirect field-oriented control (IFOC) drives due to errors in the estimate of the rotor time constant provides a guideline for setting the gains of PI

† Corresponding Author: Center for Non-Linear Dynamics, Department of Electrical Engineering, The PNG University of Technology, LAE. (rkarthiekeyan@gmail.com)
* Center for Non-Linear Dynamics, Department of Electrical Engineering, The PNG University of Technology, LAE.
** Center for Non-Linear Dynamics, Defense University, Ethiopia.
Received: May 29, 2016; Accepted: November 3, 2017

speed controller in order to avoid Hopf bifurcation [18]. It has been proven the occurrence of either co-dimension one bifurcation such as saddle node bifurcation and Hopf bifurcation and co-dimension two such as Bogdanov-Takens or zero-Hopf bifurcation in IFOC induction motors [19-21].

## 2. Preliminaries of the Wind Turbine Generator

The Aerodynamic model of wind turbine is given by [5],

$$P_w = \frac{1}{2}\rho\pi R^2 v_w^3 c_p \tag{1}$$

$\rho = Air$ Density
$R = Turbine$
$v_w = Wind$ velocity
$c_p = Power$ coefficient representing the aerodynamic efficiency
$c_i = Drag$ coefficient

Here we assume $c_i \rightarrow$ Constant

$$c_p(\lambda,\beta) = c_1\left(c_2\left(\frac{1}{\lambda+0.05\beta}-\frac{0.035}{\beta^3+1}\right)-c_3\beta-c_4\right) \times e^{-\left(\frac{1}{\lambda+0.08\beta}-\frac{0.035}{\beta^3+1}\right)}+c_6\lambda \tag{2}$$

where
$\lambda \rightarrow Tip$ speed ratio, $\beta \rightarrow$ Pitch angle
$c_1 = 0.5109; c_2 = 116; c_3 = 0.4; c_4 = 5; c_5 = 21; c_6 = 0.068$

$$\lambda = \frac{\omega R}{v_w} \tag{3}$$

where $\omega \rightarrow Rotor$ angular speed and $\lambda=\lambda_{opt}$
Solving (2) and (3) in (1),

$$P_{opt} = \frac{1}{2}\rho\pi R^2 c_{p\max}\left[\left(\frac{R}{\lambda_{opt}}\right)\omega\right]^3 \tag{4}$$

For deriving the model of Permanent Magnet Synchronous Generator (PMSG), we start deriving the basic voltage equations and iterate the basic equations,
(a) $3\phi$ ABC stationary to two phase a and $\psi$ stationary frame

$$\begin{aligned} v_\alpha &= v_a - \frac{1}{2}v_b - \frac{1}{2}v_c \\ v_\psi &= \frac{\sqrt{3}}{2}v_b - \frac{\sqrt{3}}{2}v_c \end{aligned} \tag{5}$$

(b) $2\phi$ a and $\psi$ stationary to two $\phi$ phase synchronous rotation reference frame

$$\begin{aligned} v_d &= v_\alpha\cos\theta + v_\psi\sin\theta \\ v_q &= -v_\alpha\sin\theta + v_\psi\cos\theta \end{aligned} \tag{6}$$

To derive the final speed and current dynamics of the PMSG we continue Iteration of convergence and repeat (5) and (6) to get,

$$\begin{aligned} \dot{\omega} &= \frac{p}{J}\left[\phi_f\dot{i}_q + (L_d - L_q)i_d i_q\right] - \frac{F}{J}\omega - \frac{T_L}{J} \\ \dot{\hat{i}}_q &= -\frac{R_s}{L_q}i_q + \frac{L_d}{L_q}\rho\omega i_d - \frac{\rho\phi_f}{L_q}\omega + \frac{v_q}{L_d} \\ \dot{\hat{i}}_d &= -\frac{R_s}{L_d}i_d + \frac{L_q}{L_d}\rho\omega i_q + \frac{v_d}{L_d} \end{aligned} \tag{7}$$

where $u_q$ and $u_d$ are quadrature and direct axis stator control voltages, $i_q$ and $i_d$ are quadrature and direct axis stator control currents, $L_q$ and $L_d$ quadrature and direct axis stator control inductances, $p$ is the number of pole pairs, $R_s$ is the stator resistance, $\phi_f$ is the rotor flux linkage with stator, $T_L$ is the Load torque, $J$ is the rotor moment of inertia, $f$ is the friction coefficient.
By simplifying

$$\begin{aligned} \dot{\hat{w}} &= a(\hat{i}_q - \hat{w}) + \varepsilon\hat{T}_d\hat{i}_q - \hat{T}_L \\ \dot{\hat{T}}_q &= -\hat{i}_q - \hat{w}\hat{i}_d + b\hat{w} + \hat{v}_q \\ \dot{\hat{T}}_d &= -\hat{i}_d + \hat{w}\hat{i}_q + \hat{v}_d \end{aligned} \tag{8}$$

where

$$\begin{aligned} &\varepsilon = \frac{\rho b L_q^{\,2}k^2(L_q - L_d)}{JR_s^{\,2}}; \quad b = \frac{-\phi_f}{kL_q}; \\ &a = \frac{fL_q}{R_s J}; \ \ \mathrm{b}=\frac{L_q}{L_d}; \ \ \mathrm{k}=\frac{fR}{L_q p\phi_f}; \hat{i}_d = \frac{L_d p\phi_f}{R_s}i_d; \\ &\hat{\mathrm{i}}_q = \frac{L_q p\phi_f}{fR_s}i_q; \hat{w} = \frac{L_q}{R_s}w; \ \ v_d = \frac{1}{R_s k}v_d; \\ &\hat{u}_q = \frac{1}{R_s k}v_q; \ \ \hat{\mathrm{T}}=\frac{L_q^{\,2}}{JR_s^{\,2}}T_L; t = \frac{R_s t'}{L_q} \end{aligned} \tag{9}$$

To derive the dimensionless state vector model of (8), let us assume $x_0 = \hat{w}$; $\mathrm{y}=\hat{\mathrm{T}}_q$; $\mathrm{z}=\hat{\mathrm{T}}_d$,

$$\begin{aligned} \dot{x} &= a(y - x) + \hat{T}_L + \varepsilon zy \\ \dot{y} &= -y - xz + bx + \hat{v}_q \\ \dot{z} &= -z + xy + \hat{v}_d \end{aligned} \tag{10}$$

The study found that the PMSG is experiencing chaotic

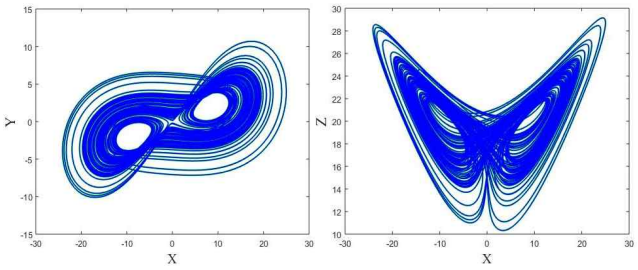

(a) (b)

**Fig. 1**. State portrait of the Fractional order PMSG system (a: XY plane, b: XZ plane)

behavior when the operating parameters $a$, $b$ and $\varepsilon$ falls in to certain area and the external inputs are set to zero, namely, $\hat{T} = \hat{v}_d = \hat{v}_q = 0$. The values of $a$, $b$ and $\varepsilon$ are a=5.45, b=20,$\varepsilon$=1. The modified equation of PMSG is given by (11) and the chaotic attractor of PMSG system is given in figure 1.

$$\begin{aligned} \dot{x} &= a(y-x) + \varepsilon zy \\ \dot{y} &= -y - xz + bx \\ \dot{z} &= -z + xy \end{aligned} \tag{11}$$

## 3. Fractional Order PMSG Model (FOPMSG):

The fractional-order differential operator is the generalization of integer-order differential operator. There are three commonly used definition of the fractional-order differential operator, viz. Grunwald-Letnikov, Riemann-Liouville and Caputo [24-26].

The fractional order model of PMSG is derived from (1) with the Caputo fractional order definition, which is defined as

$$D_t^{\alpha} f(t) = \frac{1}{\Gamma(1-\alpha)} \int_{t_0}^{t} \frac{\dot{f}(\tau)}{(t-\tau)^{\alpha}} d\tau \tag{12}$$

where $\alpha$ is the order of the system $t_0$ and $t$ are limits of the fractional order equation, $f(t)$ is integer order calculus of the function.

For numerical calculations we use Caputo via Riemann-Liouville fractional derivative [27] and the above equation is modified as

$${}_{(t-L)}D_t^{\alpha} f(t) = \lim_{h \to 0} \left\{ h^{-\alpha} \sum_{j=0}^{N(t)} b_j \left( f(t-jh) \right) \right\} \tag{13}$$

Theoretically fractional order differential equations use infinite memory. Hence when we want to numerically calculate or simulate the fractional order equations we have to use finite memory principal, where $L$ is the memory length and $h$ is the time sampling.

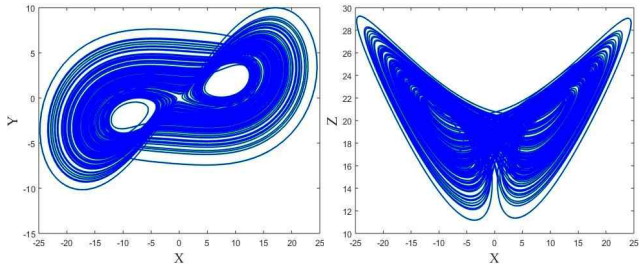

(a) (b)

**Fig. 2**. State portrait of the Fractional order PMSG system (a: XY plane, b: XZ plane,)

$$\begin{aligned} N(t) &= \min\left\{ \left[ \frac{t}{h} \right], \left[ \frac{L}{h} \right] \right\} \\ b_j &= \left( 1 - \frac{\alpha + \alpha}{j} \right) b_{j-1} \end{aligned} \tag{14}$$

Applying these fractional order approximations in to the integer order PMSG model (7) yields the fractional order PMSG described by (15),

$$\begin{aligned} D_t^{q_1} w &= \frac{p}{J}(\phi_f i_q + (L_d - L_q) i_d i_q) - \frac{f}{J} w - \frac{T_L}{J} \\ D_t^{q_2} i_q &= -\frac{R_s}{L_q} i_q + \frac{L_d}{L_q} pw i_d - \frac{p\phi_f}{L_q} w + \frac{u_q}{L_d} \\ D_t^{q_3} i_d &= -\frac{R_s}{L_d} i_d + \frac{L_q}{L_d} pw i_q + \frac{u_d}{L_d} \end{aligned} \tag{15}$$

Where $q_1, q_2$ and $q_3$ are the fractional orders of the respective states. To study the chaotic behavior of the PMSG fractional order model, we assume the external inputs $\hat{T} = \hat{v}_d = \hat{v}_q = 0$. To derive the dimensionless state vector model of (15), let us assume $x_0 = \hat{w}$; y=$\hat{T}_q$; z=$\hat{T}_d$.

$$\begin{aligned} D_t^{q_1} \dot{x} &= a(y-x) + \varepsilon zy \\ D_t^{q_2} \dot{y} &= -y - xz + bx \\ D_t^{q_3} \dot{z} &= -z + xy \end{aligned} \tag{16}$$

The above fractional order model exhibits chaos when a=5.45, b=20,$\varepsilon$=1. The 3D chaotic state portrait of the model (16) is shown in figure 2. The orders of the system (16) are taken as $q_1 = 0.99$, $q_2 = 0.99$, $q_3 = 0.99$. The fractional order of the equations are taken close to the integer order as its more complex to control a fractional order close to 1.

## 4. Dynamics of The Fractional Order PMSG Model:

In this section we analyze the fractional order system for

various properties of chaotic behavior like equilibria points, Lyapunov exponents, bifurcation and bicoherence.

### 4.1 Equilibria points and lyapunov exponents:

The equilibria of the system (16) can be found by solving (17).

$$\begin{aligned} 0 &= a(y-x)+\varepsilon zy \\ 0 &= -y-xz+bx \\ 0 &= -z+xy \end{aligned} \tag{17}$$

The three equilibria points of the system (2) are $E_1=(0,0,0)$ and $E_{2,3}=(b-1,\pm\sqrt{b-1},\pm\sqrt{b-1})$.

And the Jacobian matrix of the system (17) is defined as,

$$J=\begin{bmatrix} -a & a+\varepsilon z & \varepsilon y \\ -z+b & -1 & -x \\ y & x & -1 \end{bmatrix} \tag{18}$$

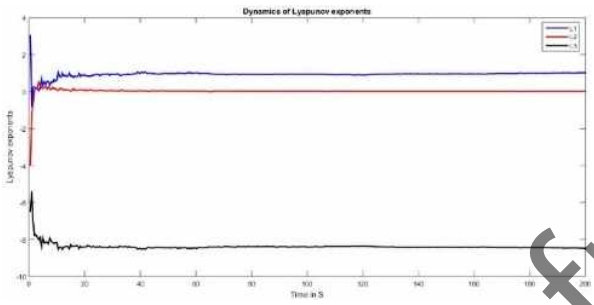


**Fig. 3**. Dynamics of Lyapunov Exponents

where $x, y \& z$ denotes the equilibrium points.

The Initial conditions are chosen as $x=3$, $y=3$ and $z=3$ and the parameter values are chosen as a=5.45, b=20,$\varepsilon$=1.

The Lyapunov exponents of the system (2) are $L1=0.852023$ $L2=0$ $L3=-8.502219$.

The Numerical results of the simulation are shown in Fig. 3

### 4.2 Bifurcation and Bicoherence:

The PMSG system shows multiple chaotic regions for variation with parameter 'a' as can be seen from figure 4. The system shows chaotic oscillations for $4\le a\le 4.4$, $4.7\le a\le 5.5$, $5.6\le a\le 5.8$ and $5.9\le a\le 7.0$. The PMSG system shows limit cycles for $4.4\le a\le 4.7$, $5.5\le a\le 5.6$ and $5.8\le a\le 5.9$. Fig. 5 shows the bifurcation of PMSG system for variation of parameter 'b' The system shows two chaotic regions $19\le b\le 19.7$ and $19.9\le b\le 21$ there exists a symmetric limit cycle region for $19.7\le b\le 19.9$. Fig. 6 shows the bifurcation of PMSG system with parameter '$\varepsilon$' the system shows more chaotic oscillation and also small bands of limit cycles. For $0\le\varepsilon\le 0.37$, $0.38\le\varepsilon\le 0.77$, $0.79\le\varepsilon\le 0.92$, $0.94\le\varepsilon\le 1.47$ and $1.7\le\varepsilon\le 2$ the system shows chaotic regions. For small bands of $0.37\le\varepsilon\le 0.38$, $0.77\le\varepsilon\le 0.79$ and $0.92\le\varepsilon\le 0.94$ wide band of $1.47\le\varepsilon\le 1.7$ the system shows multiple symmetric limit cycles.

The second most important bifurcation analysis is for the fractional order impact on the FOPMSG systems. To investigate this we vary the fractional order of the system

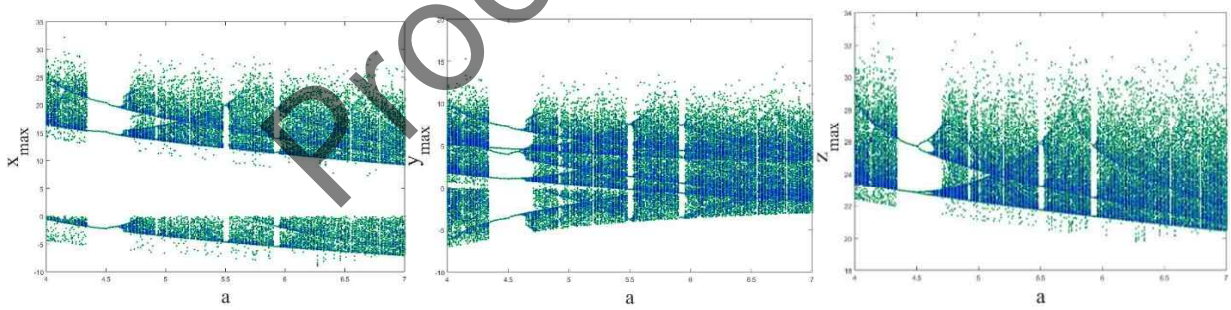


**Fig. 4**. Bifurcation of PMSG system versus *a*

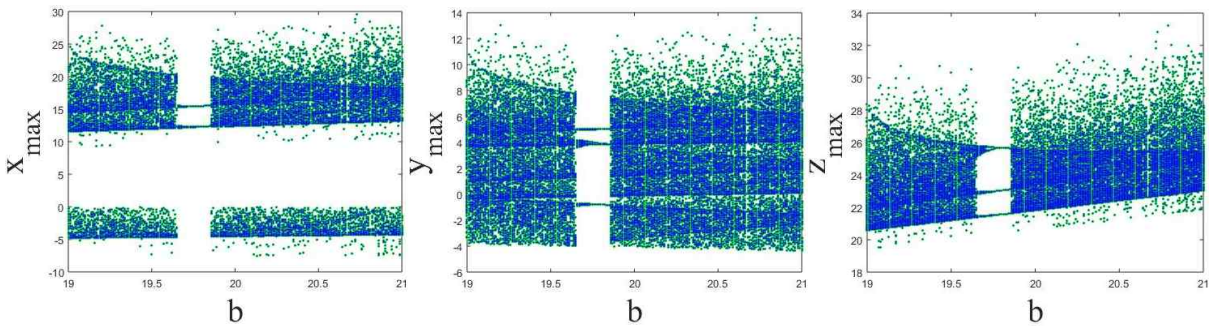


**Fig. 5**. Bifurcation of PMSG system versus *b*

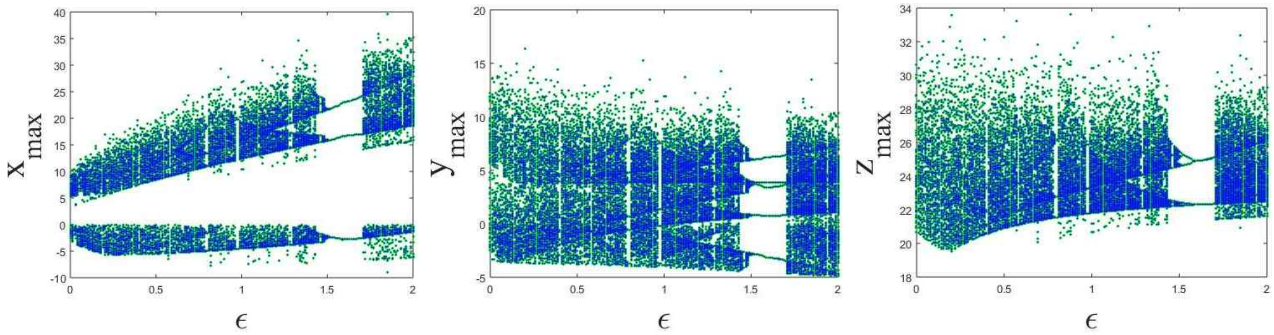


**Fig. 6**. Bifurcation of PMSG system versus $\varepsilon$

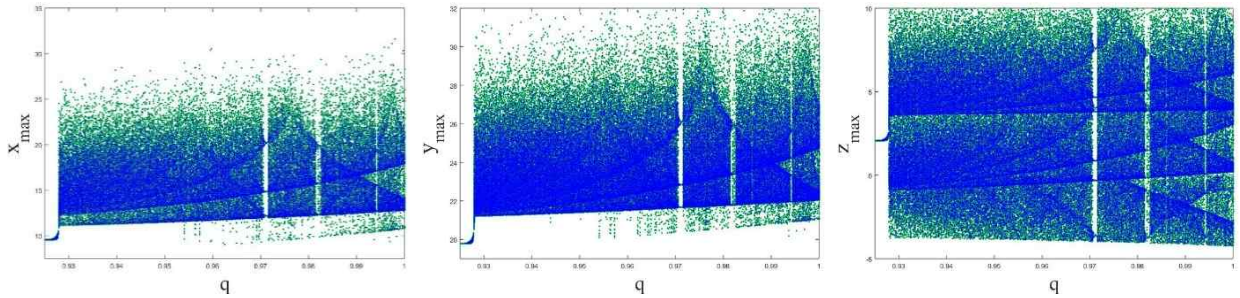


**Fig. 7**. Bifurcation plot of FOPMSG versus $q$

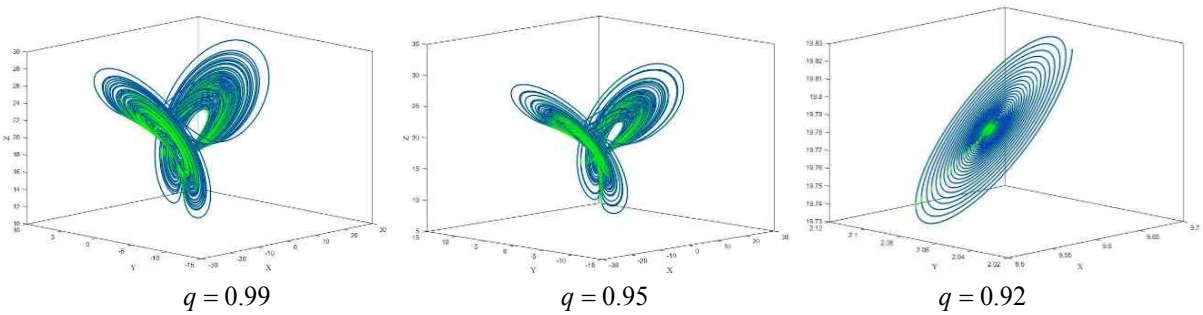


**Fig. 8**. 3D state portrait of the FOPMSG system for various fractional orders

and study the system states responses. Fig. 7 shows the fractional order bifurcation of the FOPMSG system and as can be seen from the figure, the FOPMSG system shows chaotic oscillations for $0.927 \le q \le 0.965$, $0.967 \le q \le 0.983$ and $0.985 \le q \le 1$. A small band of inverse period doubling occurs for $0.965 \le q \le 0.967$ and $0.983 \le q \le 0.985$. The system shows its maximum Lyapunov exponents for $q = 0.93$ $[L_1 = 0.9312]$ which is larger than the Lyapunov exponent of the integer order PMSG system confirming that chaotic oscillations are more in fractional order. Hence it is evident that chaos suppression in fractional order is more efficient compared to integer order chaos suppression.

The bicoherence or the normalized bispectrum is a measure of the amount of phase coupling that occurs in a signal or between two signals. Both bicoherence and bispectrum are used to find the influence of a nonlinear system on the joint probability distribution of the system input. Phase coupling is the estimate of the proportion of energy in every possible pair of frequency components $f_1, f_2, f_3 \ldots f_n$. Bicoherence analysis is able to detect coherent signals in extremely noisy data, provided that the coherency remains constant for sufficiently long times, since the noise contribution falls off rapidly with increasing $N$. The auto bispectrum of a chaotic system is given by Pezeshki [23]. He derived the auto bispectrum with the Fourier coefficients.

$$B(\omega_1, \omega_2) = E[A(\omega_1)A(\omega_2)A^*(\omega_1 + \omega_2)] \tag{19}$$

where $\omega_n$ is the radian frequency and $A$ is the Fourier coefficients of the time series. The normalized magnitude spectrum of the bispectrum known as the squared bicoherence is given by

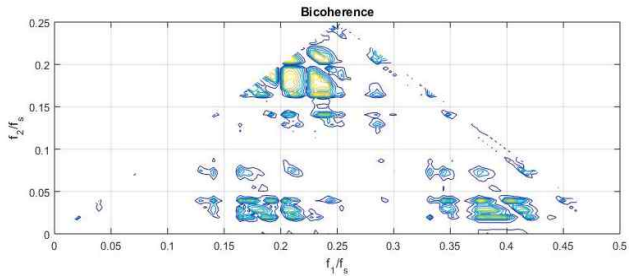


**Fig. 9**. Bicoherence of the state $x$ of Fractional order System (16)

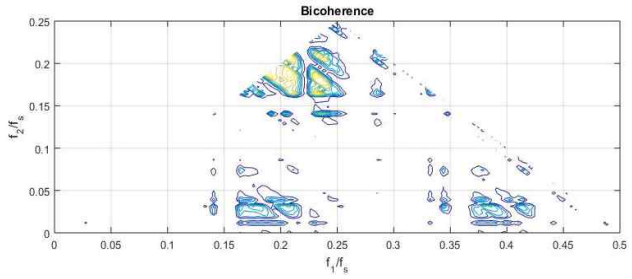


**Fig. 10**. Bicoherence of the state $y$ of Fractional order System (16)

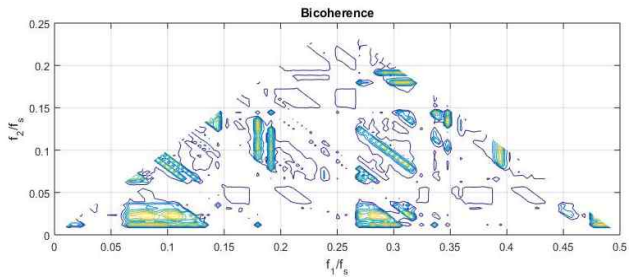


**Fig. 11**. Bicoherence of the state $z$ of Fractional order System (16)

$$b(\omega_1,\omega_2)=\frac{\left|B(\omega_1,\omega_2)\right|^2}{P(\omega_1)P(\omega_2)P(\omega_1+\omega_2)} \tag{20}$$

where $P(\omega_1)$ and $P(\omega_2)$ are the power spectrums at $f_1$ and $f_2$.

Figs. 9-11 shows the bicoherence contours of all the states together. Shades in yellow represent the multi-frequency components contributing to the power spectrum. From figures 9-11 the cross-bicoherence is significantly non zero, and non-constant, indicating a nonlinear relationship between the states. The yellow shades and non-sharpness of the peaks, as well as the presence of structure around the origin in figures (cross bicoherence) indicates that the nonlinearity between the states $x,y,z$ are not of the quadratic nonlinearity and hence may be because of nonlinearity of higher dimensions. The most two dominant frequencies ( $f_1,f_2$ ) are taken for deriving the contour of bicoherence. The sampling frequency ( $f_s$ ) is taken as the reference frequency.

## 5. Stability analysis of FOPMSG system:

Commensurate Order: For commensurate FOPMSG system of order $q$, the system is stable and exhibits chaotic oscillations if $\left|\arg(eig(J_E))\right|=\left|\arg(\lambda_i)\right|>\frac{q\pi}{2}$ where $J_E$ is the Jacobian matrix at the equilibrium $E$ and $\lambda_i$ are the Eigen values of the FOPMSG system where $i=x,y,z$. As seen from the FOPMSG system, the Eigen values should remain in the unstable region and the necessary condition for the FOPMSG system to be stable is $q>\frac{2}{\pi}\tan^{-1}\left(\frac{\left|\mathrm{Im}\,\lambda\right|}{\mathrm{Re}\,\lambda}\right)$. As the Eigen values of the system are $\lambda_{1,2}$=-13.8998, $\lambda_3$= 7.4498, $\lambda_4$ = -1; it's clearly seen that the value $\lambda_2$ is a positive value and remains in the unstable region contributing to the existence of chaotic oscillations.

Incommensurate Order: The necessary condition for the FOPMSG system to exhibit chaotic oscillations in the incommensurate case is, $\frac{\pi}{2M}-\min_i\left(\left|\arg(\lambda i)\right|\right)>0$ where $M$ the LCM of the fractional orders. If $q_1=0.95$, $q_2=0.94, q_3=0.93$, then $M=100$. The characteristic equation of the system evaluated at the equilibrium is, $\det(diag[\lambda^{Mq_1},\ \lambda^{Mq_2},\ \lambda^{Mq_3}]-J_E)=0$ and by substituting the values of $M$ and the fractional orders, $\det(diag[\lambda^{95},\ \lambda^{94},\ \lambda^{93}]-J_E)=0$ the characteristic equation is, $\lambda^{282}+\lambda^{190}+2\lambda^{189}+\ 5.45\lambda^{187}+\lambda^{97}+3\lambda^{96}+8.45\lambda^{95}+1.19\lambda^{94}\ -103.55\lambda^{93}+\lambda^3\ +7.45\lambda^2-97.1\lambda-103.55$ The approximated solution of the characteristic equation is $\lambda_{282}=-2.5419$ and whose argument is zero and which is the minimum argument and hence the stability necessary condition becomes, $\frac{\pi}{20}-0>0$ which solves for $0.1571>0$ and hence the FOPMSG system is stable and chaos exists in the incommensurate system.

## 6. Chaos Suppression of the Fractional Order System Using Fractional Order Adaptive Controller:

The design goal of this paper is to design a Fractional order adaptive controller to suppress the chaotic oscillations in system (16). The system (16) with the adaptive controller $u_x$ is derived as follows,

$$\begin{aligned} D_t^{q_1}\dot{x}&=a(y-x)+\varepsilon zy+u_x\\ D_t^{q_2}\dot{y}&=-y-xz+bx+u_y\\ D_t^{q_3}\dot{z}&=-z+xy+u_z \end{aligned} \tag{21}$$

To control the chaotic oscillations, we define the controllers as,

$$\begin{aligned} u_x &= -\hat{a}(t)(y-x) + \hat{\varepsilon}(t)zy - k_x x \\ u_y &= y + xz - \hat{b}(t)x - k_y y \\ u_z &= z - xy - k_z z \end{aligned} \tag{22}$$

where $\hat{a}$, $\hat{b}$ and $\hat{\varepsilon}$ are the parameter estimates of the uncertain parameters and $k_x, k_y \text{ and } k_z$ are positive constants. The parameter estimation errors are defines as,

$$\begin{aligned} e_a &= a - \hat{a}(t) \\ e_b &= b - \hat{b}(t) \\ e_\varepsilon &= \varepsilon - \hat{\varepsilon}(t) \end{aligned} \tag{23}$$

The fractional derivative of the parameter estimation errors are given by,

$$\begin{aligned} D^{q_1} e_a &= -D^{q_1}\hat{a}(t) \\ D^{q_2} e_b &= -D^{q_2}\hat{b}(t) \\ D^{q_1} e_\varepsilon &= -D^{q_1}\hat{\varepsilon}(t) \end{aligned} \tag{24}$$

## 7. Stability Analysis of the Adaptive Fractional Order Controller:

In order to analyze the stability of the designed control algorithm we use Lyapunov stability theory. The Lyapunov function for the controller (22) and system (16) can be given by (25)

$$V = \frac{1}{2}\left(x^2 + y^2 + z^2 + e_a^2 + e_b^2 + e_\varepsilon^2\right) \tag{25}$$

$$V = x\dot{x} + y\dot{y} + z\dot{z} + e_a\dot{e}_a + e_b\dot{e}_b + e_\varepsilon\dot{e}_\varepsilon \tag{26}$$

By definition of fractional calculus [22, 23],

$$\dot{x}(t) = D_t^{1-q} \cdot D_t^q x(t) \tag{27}$$

Substituting in (26),

$$\begin{aligned} V = {} & xD_t^{1-q}\cdot D_t^q x + yD_t^{1-q}\cdot D_t^q y \\ & + zD_t^{1-q}\cdot D_t^q z + e_a D_t^{1-q}\cdot D_t^q e_a \\ & + e_b D_t^{1-q}\cdot D_t^q e_b + e_\varepsilon D_t^{1-q}\cdot D_t^q e_\varepsilon \end{aligned} \tag{28}$$

From (28) it is clear that the calculation of the sign of the first Lyapunov derivative is very difficult. Hence we derive a new lemma to find the sign of the Lyapunov first derivative.

**a. Lemma-1:**

As defined by if $e(t)$ be a time continuous and derivable function. Then for any time instant $t \geq t_0$,

$$\frac{1}{2}D_t^\alpha e^2(t) \leq e(t) \times D_t^\alpha e(t) \; \forall \alpha \in (0,1) \tag{29}$$

Proof: To prove expression (29) is true we start with,

$$e(t)D_t^\alpha e(t) - \frac{1}{2}D_t^\alpha e^2(t) \geq 0 \; \forall \alpha \in (0,1) \tag{30}$$

By Definition

$$D_t^\alpha e(t) = \frac{1}{\Gamma(1-\alpha)}\int_{t_0}^{t} \frac{\dot{e}(\tau)}{(t-\tau)^\alpha} d\tau \tag{31}$$

$$\frac{1}{2}D_t^\alpha e^2(t) = \frac{1}{\Gamma(1-\alpha)}\int_{t_0}^{t} \frac{e(\tau)\cdot\dot{e}(\tau)}{(t-\tau)^\alpha} d\tau \tag{32}$$

Modifying (32),

$$\frac{1}{\Gamma(1-\alpha)}\int_{t_0}^{t} \frac{e(t)\cdot\dot{e}(\tau) - e(\tau)\dot{e}(\tau)}{(t-\tau)^\alpha} d\tau \geq 0 \tag{33}$$

Let us assume,

$$E(\tau) = e(t) - e(\tau) \;\&\; \dot{E}(\tau) = -\dot{e}(\tau) \tag{34}$$

Substitute (34) in (33)

$$\frac{1}{\Gamma(1-\alpha)}\int_{t_0}^{t} \frac{E(\tau)\dot{E}(\tau)}{(t-\tau)^\alpha} d\tau \geq 0 \tag{35}$$

Integration (35) by parts

$$\frac{1}{\Gamma(1-\alpha)}(t-\tau)^{-\alpha}\cdot\frac{1}{2}E^2(\tau) - \int_{t_0}^{t}\frac{1}{2}E^2(\tau)\cdot\left(\frac{\alpha(t-\tau)^{-\alpha-1}}{\Gamma(1-\alpha)}\right) \leq 0 \tag{36}$$

$$\begin{aligned} & \left[\frac{E^2(\tau)}{2\Gamma(1-\alpha)(t-\tau)^\alpha}\right]_{\tau=t} - \left[\frac{E^2(t_0)}{2\Gamma(1-\alpha)(t-t_0)^\alpha}\right] \\ & \qquad - \frac{1}{2}\frac{\alpha}{\Gamma(1-\alpha)}\int_{t_0}^{t}\frac{E^2(\tau)}{(t-\tau)^{\alpha+1}} d\tau \leq 0 \end{aligned} \tag{37}$$

Solving first term of (37) for $\tau = t$

$$\begin{aligned} \lim_{\tau\to t}\frac{E^2(\tau)}{2\Gamma(1-\alpha)(t-\tau)^\alpha} &= \frac{1}{2\Gamma(1-\alpha)}\lim_{\tau\to t}\frac{\begin{bmatrix} e^2(t)+e^2(\tau) \\ -2e(t)\cdot e(\tau)\end{bmatrix}^2}{(t-\tau)^\alpha} \\ &= \frac{1}{2\Gamma(1-\alpha)}\lim_{\tau\to t}\begin{bmatrix} -2e(t)\dot{e}(\tau) + \\ 2e(\tau)\cdot\dot{e}(\tau) \\ -\alpha(t-\tau)^{\alpha-1}\end{bmatrix} = 0 \end{aligned} \tag{38}$$

Eq. (38) can be rewritten as

$$\frac{E^2(t_0)}{2\Gamma(1-\alpha)(t-t_0)^{\alpha}}+\frac{\alpha}{2\Gamma(1-\alpha)}\int_{t_0}^{t}\frac{E^2(\tau)}{(t-\tau)^{\alpha+1}}d\tau\geq 0 \quad (39)$$

which clearly holds as $\alpha$ lies between $0\leq\tau\leq 1$, the r.h.s of the Eq. (39) will always be a positive value and hence Proved.

---

Substituting (29) in (25) and solving for the Lyapunov first derivative,

$$\begin{aligned}\dot{V}&=e_a[x(y-x)-\dot{\hat{a}}]+e_\varepsilon[xyz-\dot{\hat{\varepsilon}}]\\&\quad+e_b[xy-\dot{\hat{b}}]-k_x x^2-k_y y^2-k_z z^2\end{aligned} \quad (40)$$

Let us define the parameter update laws as,

$$\begin{aligned}\dot{\hat{a}}&=x(y-x)\\\dot{\hat{b}}&=xy\\\dot{\hat{\varepsilon}}&=xyz\end{aligned} \quad (41)$$

Substituting (41) in (40),

$$\dot{V}=-k_x x^2-k_y y^2-k_z z^2 \quad (42)$$

which is clearly a negative semidefinite function and hence the control scheme proposed by this paper proves to be stable with a origin.

## 8. Chaos Suppression of the Fractional Order System Using Adaptive Sliding Mode Control (FOASMC):

The control goal of this paper is to design a suitable adaptive sliding mode controller for suppression of chaotic oscillations in the fractional order PMSG system (21). For deriving the robust ASMC controller for the system (21), let us redefine the fractional order system with a sliding mode controller $u(t)$ as in (21)

Let us define the integral sliding mode surface as,

$$\begin{aligned}s_x&=x+k_x\int_0^t x(\tau)d\tau\\s_y&=y+k_y\int_0^t y(\tau)d\tau\\s_z&=z+k_z\int_0^t z(\tau)d\tau\end{aligned} \quad (43)$$

The parameter estimation errors are defined as,

$$\begin{aligned}e_a&=\hat{a}-a\\e_b&=\hat{b}-b\\e_\varepsilon&=\hat{\varepsilon}-\varepsilon\end{aligned} \quad (44)$$

The fractional derivative of the estimation error is,

$$\begin{aligned}D^q e_a&=D^q\hat{a}\\D^q e_b&=D^q\hat{b}\\D^q e_\varepsilon&=D^q\hat{\varepsilon}\end{aligned} \quad (45)$$

The fractional derivatives of the sliding surface (43) is,

$$\begin{aligned}D^{q_1}s_1&=D^{q_1}x_1+k_1x_1\\D^{q_2}s_2&=D^{q_2}x_2+k_2x_2\\D^{q_3}s_3&=D^{q_3}x_3+k_3x_3\\D^{q_4}s_4&=D^{q_4}x_4+k_4x_4\end{aligned} \quad (46)$$

Let us consider the following Lyapunov function,

$$V=\frac{1}{2}\left[s_x^2+s_y^2+s_z^2+e_a^2+e_b^2+e_\varepsilon^2\right] \quad (47)$$

The first derivative of the Lyapunov candidate function is,

$$\dot{V}=s_1\dot{s}_1+s_2\dot{s}_2+s_3\dot{s}_3+e_a\dot{e}_a+e_b\dot{e}_b+e_\varepsilon\dot{e}_\varepsilon \quad (48)$$

By definition of fractional calculus [40, 41], we obtain

$$\dot{x}(t)=D_t^{1-q}\cdot D_t^q x(t) \quad (49)$$

Applying (49) in (48)

$$\begin{aligned}\dot{V}&=s_x D_t^{1-q}\cdot D_t^q s_x+s_y D_t^{1-q}\cdot D_t^q s_y+s_z D_t^{1-q}\cdot D_t^q s_z\\&\quad+e_a D_t^{1-q}\cdot D_t^q e_a+e_b D_t^{1-q}\cdot D_t^q e_b+e_\varepsilon D_t^{1-q}\cdot D_t^q e_\varepsilon\end{aligned} \quad (50)$$

Thus, it is clear that stability calculations with (50) are very difficult. So, we used lemma 1 to solve (50)

Let $e(t)$ be a time continuous and derivable function. As proved in lemma 1, for any time instant $t\geq t_0$, we have

$$\frac{1}{2}\mathrm{D}_\mathrm{t}^q x^2(\mathrm{t})\quad \forall x(\mathrm{t})\times \mathrm{D}_\mathrm{t}^q x(\mathrm{t})\quad \forall q\in(0,1) \quad (51)$$

Using (51) in (50)

$$\begin{aligned}\dot{V}&=s_x\left[D^{q_1}x+k_x x\right]+s_y\left[D^{q_2}y+k_y y\right]\\&\quad+s_z\left[D^{q_3}z+k_z z\right]+e_a D^q\hat{a}+e_b D^q\hat{b}+e_\varepsilon D^q\hat{\varepsilon}\end{aligned} \quad (52)$$

Let us define the adaptive controllers as,

$$\begin{aligned}u_x(t)&=-\hat{a}(y-x)-\hat{\varepsilon}zy-k_x x-\eta_x\,\mathrm{sgn}(s_x)-\rho_x s_x\\u_y(t)&=y+xz-\hat{b}x-k_y y-\eta_y\,\mathrm{sgn}(s_y)-\rho_y s_y\\u_z(t)&=z-xy-k_z x_z-\eta_z\,\mathrm{sgn}(s_z)-\rho_z s_z\end{aligned} \quad (53)$$

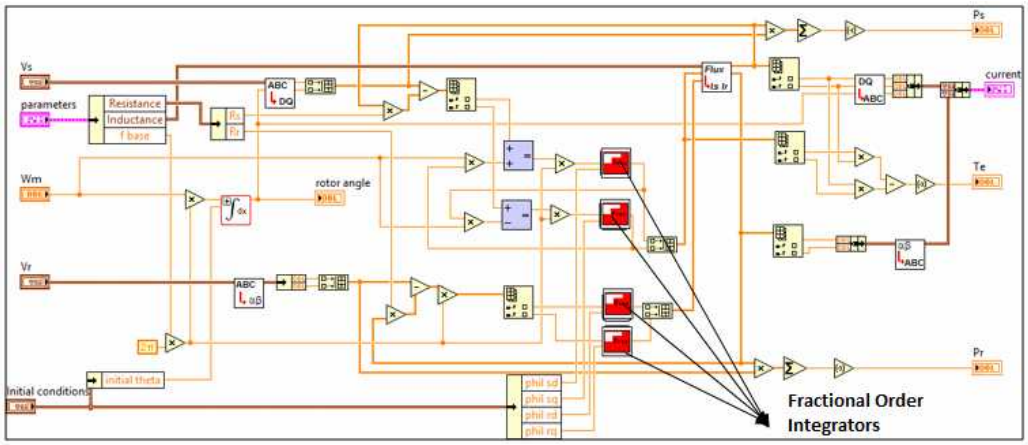


**Fig. 12**: Fractional order PMSG Model implementation

And the parameter estimation law as,

$$\begin{aligned} D^q \hat{a} &= s_x (y - x) \\ D^q \hat{b} &= s_y x \\ D^q \hat{\varepsilon} &= s_x z y \end{aligned} \tag{54}$$

By applying parameter update law (54) and adaptive controllers (53) in (52)

$$\begin{aligned} \dot{V} \le & -\eta_x |s_x| - \eta_y |s_y| - \eta_z |s_z| \\ & - \rho_x s_x^2 - \rho_y s_y^2 - \rho_z s_z^2 - \end{aligned} \tag{55}$$

As $\rho_i$ and $\eta_i$ are positive for $i = x, y, z$ , the Lyapunov first derivative (55) is a negative definite function which infers that the controller is stable and is valid for any bounded initial conditions.

## 9. Numerical Simulations and Discussions

A control strategy based on fractional-order adaptive nonlinear controllers are considered for the chaos suppression in wind turbines with PMSG. We used LabVIEW with Control and Simulation loop for analyzing the numerical simulation results. The PMSG parameters for simulation are as follows, Type PMSG, 2.0 MW, 690 V, 9.75 Hz, non-salient pole, Rated Mechanical Power -2.0 MW, Rated Apparent Power -2.2419 MVA, Rated Power Factor -0.8921, Rated Rotor Speed -22.5 r/min, Number of Pole Pairs -26, Rated Mechanical Torque- 848826 Nm, Rated Rotor Flux Linkage- 5.8264 (rms), Stator Winding Resistance- 0.821, d axis Synchronous Inductance- 1.5731, q axis Synchronous Inductance -1.5731. For the adaptive control algorithm we implement the proposed nonlinear controller from (22) with parameter update law (41) is implemented in LabVIEW and investigated for its performance. Fig. 12 shows the design of the PMSG model in LabVIEW. The parameters for the design are taken as discussed above. Fig. 13 shows the proposed control scheme implemented with fractional order controllers. The PI blocks defined in the control scheme are the fractional nonlinear controllers proposed in (21) & (42). Fig. 10 shows the chaos control of the fractional order PMSG model. The controller is switch on at $t = 140s$ .

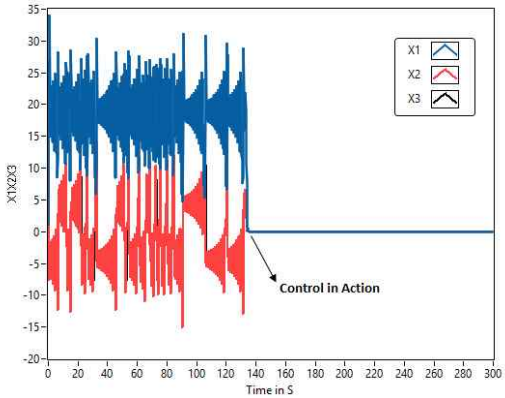


**Fig. 13**: Chaos suppression in PMSG ( $t = 140s$ )

Then the second algorithm, the Fractional order PMSG system (21) with the robust adaptive sliding mode controller (26) is implemented in FPGA for realization and validation. The initial conditions are chosen as in $[3,3,3]$ and the parameter values are chosen as $[0,6,2]$ . The fractional orders of the system (14) are chosen as commensurate $q = 0.93$ . The state trajectories of the controlled fractional-order PMSG system are shown Fig. 10, where the controller is switched at $t = 10s$ . Fig. 11, shows the parameter estimate with controller in action from $t = 0.1s$ . It can be clearly observed that the state trajectories converges to zero as soon as the controller is introduced which clearly shows that the fractional order system is well-controlled by the adaptive controller with the uncertainty.

## 10. FPGA Implementation of the FOPMSG and FOASMC Controllers:

In this section we discuss about the implementation of the proposed FOPMSG systems in FPGA [28, 29] using the Xilinx (Vivado) System Generator. The implementation of fractional order integrators play a crucial role in the designing of controllers for FOPMSG systems and we use the finite approximation technique [28, 29] and configure the memory registers for the binomial coefficients [28] using the mathematical relation discussed in (12), (13) and (14) and the value of h is taken as $0.001$ and the initial conditions are fed in to the forward register with fractional order taken as $q = 0.93$. Fig. 14 shows the FPGA implementation of FOPMSG system and Table 1 shows the resources utilised by the FOPMSG system including the clock frequency. Then we implement the fractional order adaptive sliding mode controllers in FPGA.

**Table 1**. Resource utilization of FOPMSG system

| Resource | Utilization | Available | Utilization % | Clock frequency | |
|---|---|---|---|---|---|
| | | | | $f_{max}$ | Used |
| LUT | 774 | 101400 | 0.76 | 300Mhz | 134Mhz |
| FF | 192 | 202800 | 0.09 | 500Mhz | 192Mhz |
| DSP | 12 | 600 | 2.00 | 250Mhz | 99Mhz |
| IO | 97 | 285 | 34.04 | 300Mhz | 95Mhz |
| BUFG | 1 | 32 | 3.13 | 300Mhz | 47Mhz |

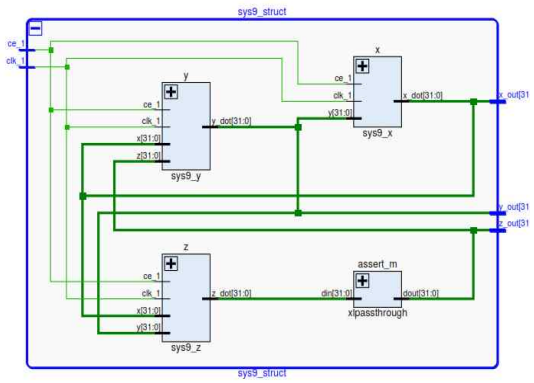


**Fig. 14**. RTL schematics for the FOPMSG system

**Table 2**: Resource utilization of FOPMSG system

| Resource | Utilization | Available | Utilization % | Clock frequency | |
|---|---|---|---|---|---|
| | | | | Available | Available |
| LUT | 2696 | 101400 | 2.66 | 500Mhz | 500Mhz |
| LUTRAM | 4 | 35000 | 0.01 | 300Mhz | 300Mhz |
| FF | 4959 | 202800 | 2.45 | 500Mhz | 500Mhz |
| DSP | 28 | 600 | 4.67 | 250Mhz | 250Mhz |
| IO | 129 | 285 | 45.26 | 300Mhz | 300Mhz |
| BUFG | 1 | 32 | 3.13 | 300Mhz | 300Mhz |

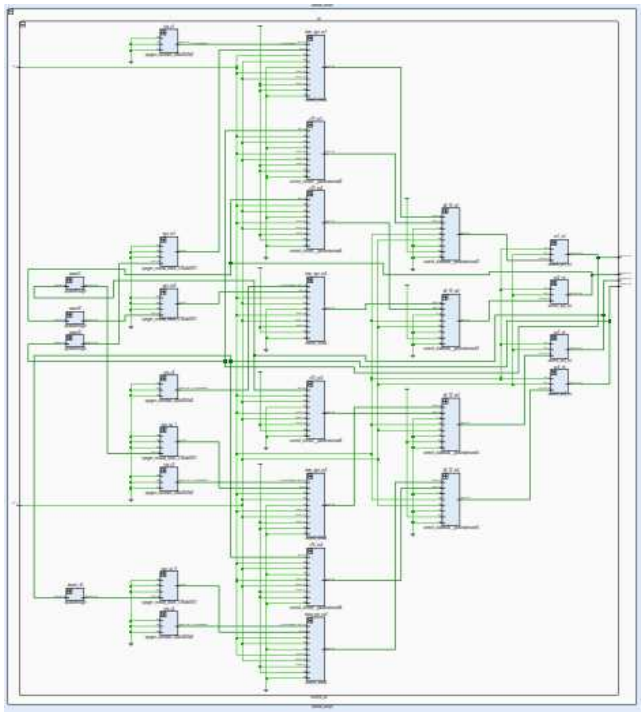

**Fig. 16.** Xilinx RTL schematics of the Sliding surfaces with the fractional integrators

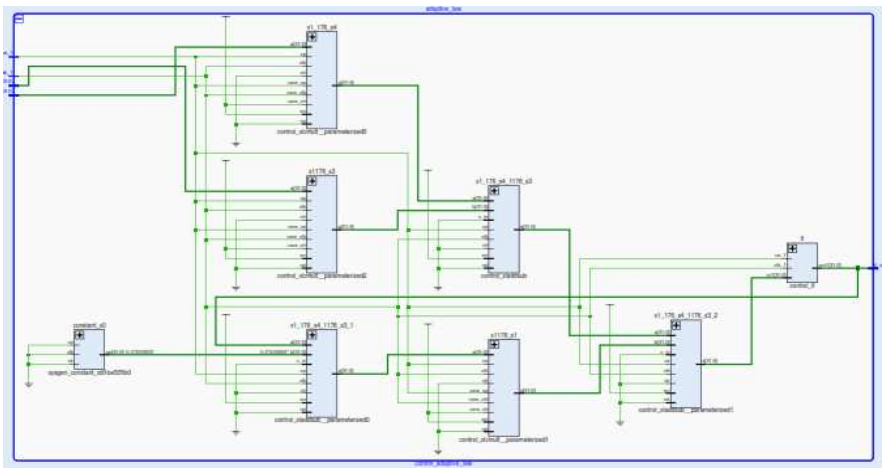

**Fig. 15.** RTL schematics of the FOASM controllers with parameter update laws

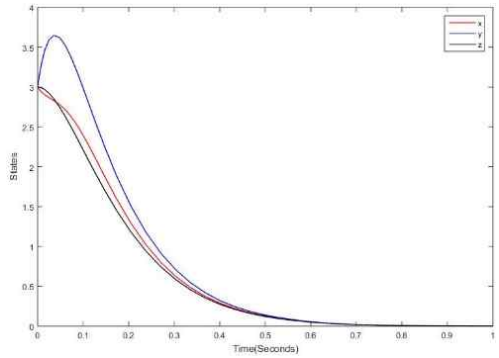


**Fig. 17**. Stabilized states of PMSG system with ASMC controllers

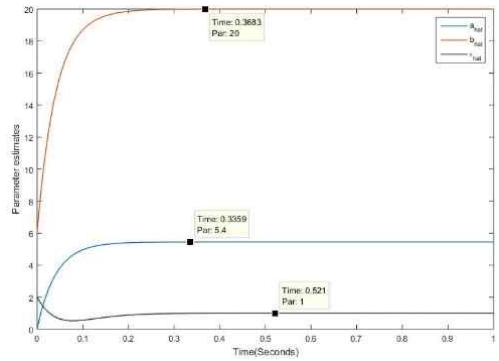


**Fig. 18**. Estimated parameters of PMSG system with ASMC controllers

Fig. 15 shows the FOASMC controllers implemented in FPGA and table 2 shows the resource utilisation. The sampling rate of the FPGA blocks play a crucial role in the existence of Lyapunov exponents and also increasing the sampling time period in some implementations may lead to a clock frequency mismatch. The performance on FPGA is directly related to the number of threads and its performances and hence the controllers for the systems are designed as four parallel threads. The fractional-order operators are implemented as building blocks and the so-called "frame delay" is not noticeable in the FPGA hardware implementation due to its parallel data structure, unlike a microprocessor-based implementation. The initial conditions are chosen as in $[3,3,3]$ and the parameter values are chosen as $[0,6,2]$. The fractional orders of the system (14) are chosen as commensurate $q = 0.93$. The controller gains are taken as $k_x = 10,\ k_y = 10,\ k_z = 10$ with sliding gains $\eta_i = 0.1$ and $\rho_i = 10$ where $i = x, y, z.$ Fig. 17 shows the stabilized states of the FOPMSG system and Fig. 18 shows the estimated parameters.

## 11. Conclusion

This paper investigates control of three-dimensional non-autonomous fractional-order uncertain model of a permanent magnet synchronous generator (PMSG) via a adaptive control technique. Firstly the dimensionless fractional order model of the PMSG is derived from the integer order model discussed in the literature using the Caputo fractional calculus. In order to study the effects of variation of parameters on the fractional order system's performance, we have investigated the bifurcation analysis of fractional order system. It is also shown that the fractional order PMSG are not only prone to instability due to Hopf bifurcation, it also exhibits limit cycles and chaos due to Bifurcation other than Hopf bifurcation which is shown by the bicoherence plots. This bispectrum analysis helps us in choosing the appropriate parameters for the proper working of the motor. As understood from the dynamic analysis of the fractional order system, it is seen that chaos oscillations are exhibited for a particular selection of parameters. To suppress such chaotic oscillations, we have derived a adaptive control technique assuming that the operating parameters of the fractional order system are unknown. The direct Lyapunov stability analysis of the robust controller is difficult and hence we have derived a new lemma to analyze the stability of the system. The proposed lemma is introduced in the Lyapunov first derivative and thus the parameter estimates are derived. We have also proved with numerical simulations that for the derived adaptive controller and the parameter update law, the origin of the system for any bounded initial conditions is asymptotically stable.

## References

[1] Mike Robinson, Paul Veers, Wind Turbine Control Workshop, Santa Clara University, Santa Clara, CA, June, 1997.

[2] S.A. Salle, D. Reardon, W.E. Leithead, M.J. Grimble, Review of wind turbine control, *Int. J. Control*, 52 (6) (1990) 1295}1310.

[3] E. Muljadi, C.P. Buttereld, P. Migliore, Variable speed operation of generators with rotor-speed feedback in wind power applications, Fifteenth ASME Wind Energy Symposium, Houston, Texas, 1996.

[4] R. Lina, L. Fucai and J. Yafei, "Active Disturbance Rejection Control for chaotic permanent magnet synchronous generator for wind power system," Control Conference (CCC), 2012 31st Chinese, Hefei, 2012, pp. 6878-6882.

[5] Manal Messadi, Adel Mellit, Karim Kemih and Malek Ghanes, Predictive control of a chaotic permanent magnet synchronous generator in a wind turbine system, *Chinese Physics B*, vol. 24, no. 1, 2015.

[6] Chih-Hong Lin, Dynamic control for permanent magnet synchronous generator system using novel modified recurrent wavelet neural network,*Nonlinear Dynamics*, vol. 77, no. 4, pp. 1261-1284, 2014.

[7] Li Z, Park J B, Joo Y H, Zhang B and Chen G "Bifurcations and chaos in a permanent-magnet

synchronous motor," *IEEE Trans. Circuits and Systems I Theory and Applications*, 49 383-387. 2002.
[8] Z. J. Jing, C. Yu and G. R. Chen, "Complex dynamics in a permanent-magnet synchronous motor model," *Chaos, Solitons and Fractals,* vol. 22, no. 4, pp. 831-848, 2004.
[9] R. L. Bagley and R. A. Calico, "Fractional order state equations for the control of viscoelastically damped structures," *Journal of Guidance, Control, and Dynamics,* vol. 14, No. 2, pp. 304-311.Koeller R C 1986 Acta Mech. 58 251, 1991
[10] Sun H H, AbdelwahadAA and Onaval B "Linear approximation of transfer function with a pole of fractional power," *IEEE transactions on automatic control* CODEN IETAA9 1984, vol. 29, no. 5, pp. 441-444 (12)., 1984
[11] Heaviside O, "Electromagnetic Theory" (New York: Chelsea), 1971
[12] Yu Y, Li H X, Wang S and Yu "Dynamic analysis of a fractional-order Lorenz chaotic system," *Chaos, Solutions & Fractals* vol.42, no. 2, pp. 1181-1189, 30 October 2009
[13] Li C G and Chen G "Chaos and hyperchaos in the fractional-order Rössler equations," *Physica A: Statistical Mechanics and its Applications*, vol. 341, pp. 55-61, 1 October 2004
[14] L¨u J G and Chen G "A note on the fractional-order Chen system," *Chaos, Solutions & Fractals,* vol. 27, no. 3, pp. 685-688, February 2006
[15] Deng W and Li C P "*Chaos synchronization of the fractional Lü system*," Physica A: Statistical Mechanics and its Applications vol. 353, pp. 61-72, 1 August 2005
[16] Mandelbort B B "The Fractal Geometry of Nature," (New York: Freeman) 427, 2006.
[17] Bazanella A.S. and R. Reginatto, "Instability Mechanisms in Indirect Field Oriented Control Drives: Theory and Experimental Results," IFAC 15th Triennial World Congress, Barcelona, Spain, 2002.
[18] Bazanella A.S. and R. Reginatto, "Instability Mechanisms in Indirect Field Oriented Control Drives: Theory and Experimental Results," IFAC 15th Triennial World Congress, Barcelona, Spain, 2002.
[19] Bazanella A.S., R. Reginatto and R.Valiatil, "Hopf bifurcations in indirect field oriented control of induction motors: Designing a robust PI controller," *Proceedings of the 38th Conference on Decision and Control*, Phoenix, Arizona USA., 1999.
[20] Reginatto .R, F. Salas, F. Gordillo and J.Aracil, "Zero-Hopf Bifurcation in Indirect Field Oriented Control of Induction Motors," First IFAC *Conference on Analysis and Control of Chaotic Systems* (CHAOS'06), 2006.
[21] Salas. F, R. Reginatto, F. Gordillo and J. Aracil, Bogdanov-Takens "Bifurcation in Indirect Field Oriented Control of Induction Motor Drives," *43rd IEEE Conference on Decision and Control*, Bahamas, 2004.
[22] Salas .F, F. Gordillo, J. Aracil and R. Reginatto, "Codimension-two Bifurcations In Indirect Field Oriented Control of Induction Motor Drives," *International Journal of Bifurcation and Chaos*, 18(3), pp. 779-792, 2008.
[23] C. Pezeshki, "Bispectral analysis of systems possessing chaotic motions," *Journal of Sound and Vibration*, vol. 137, no. 3, pp. 357-368, 1990.
[24] Li, R. H. and Chen W. S, "Fractional order systems without equilibria" *Chin. Phys. B* 2013.
[25] Petras, I. "A note on the fractional-order Chua's system," *Chaos Solitons and Fractals* 38, 140-147, 2008.
[26] Katugampola, U.N., "A New Approach To Generalized Fractional Derivatives," *Bull. Math. Anal. App*. Vol. 6, no. 4, pp. 1-15, 15 October 2014.
**[27]** Mohamed, Notes on Some Fractional Calculus Operators and Their Properties, *Journal of Fractional Calculus and Applications,* vol. 5(3S), no. 19, pp. 1-10 2014.
[28] Karthikeyan Rajagopal, Guessas Laarem, Anitha Karthikeyan, Ashokkumar Srinivasan, Girma adam, "Fractional order memristor no equilibrium chaotic system with its adaptive sliding mode synchronization and genetically optimized fractional order PID synchronization," *Complexity*, Article ID 1892618, https://doi.org/10.1155/2017/1892618, 2017
[29] Rajagopal. K, Karthikeyan. A, Srinivasan. A, "FPGA implementation of novel fractional order chaotic system with two equilibriums and no equilibrium and its adaptive sliding mode synchronization," *Nonlinear Dynamics*, DOI 10.1007/s11071-016-3189-z., 2016 synchronization," *Nonlinear Dynamics*, DOI 10.1007/s11071-016-3189-z., 2016

**Karthikeyan Rajagopal** He completed his PhD in Electronics and Communication Engineering with specializin g in Chaos-based Secure Communication Engineering. His post-graduation was in embedded system technologies with emphasis on real-time targets programming. He is presently working as an Associate Professor in Electronics Engineering and research member of Center for Nonlinear Dynamics of Defence University, Ethiopia. His present research areas include fractional order nonlinear systems and control, time delay systems, FPGA and LabVIEW implementations of fractional order systems.

**Anitha Karthikeyan** She completed her PhD in Electronics and Communication Engineering with specialization in Discrete Chaos synchronization for Secure communication Engineering. Her post-graduation was in embedded system technologies. Her research interests are FPGA implementation of fractional order systems, Discrete synchronization, time delay systems, etc.

**Prakash Duraisamy** He completed his PhD in Mechanical Engineering with specializing in Dynamic Analysis and Nonlinearity Suppression in Fractional-Order Uncertain Electro-Mechanical Systems. His post-graduation was in Computer Aided Design. His research interests are dynamic analysis of Integer order and fractional order nonlinear systems, time delay systems, design of Vibration absorbers and isolators, etc.